Turkish Journal of Electrical Engineering & Computer Sciences

http://journals.tubitak.gov.tr/elektrik/

Research Article

Turk J Elec Eng & Comp Sci
(2017) 25: 3528 – 3539

doi:10.3906/elk-1505-181

Numerical study of AC loss of two-layer HTS power transmission cables composed of coated conductors with a ferromagnetic substrate

Şükrü YILDIZ[1,*], **Fedai İNANIR**[2], **Ahmet ÇİÇEK**[3], **Fedor GÖMÖRY**[4]

[1]Department of Metallurgical and Materials Engineering, Faculty of Engineering and Architecture, Ahi Evran University, Kırşehir, Turkey

[2]Department of Physics, Faculty of Arts and Science, Yıldız Technical University, İstanbul, Turkey

[3]Department of Nanoscience and Nanotechnology, Faculty of Arts and Science, Mehmet Akif Ersoy University, Burdur, Turkey

[4]Institute of Electrical Engineering, Slovak Academy of Sciences, Bratislava, Slovakia

Received: 28.05.2015 • **Accepted/Published Online:** 03.03.2017 • **Final Version:** 05.10.2017

Abstract: This work includes the simulation of hysteretic AC losses in two-layer HTS power transmission cables made of second-generation high-temperature superconducting tapes with a ferromagnetic substrate subject to an oscillating AC transport current, calling upon the COMSOL Multiphysics finite-element software program and exploiting an AC/DC module. How the AC transport loss is influenced by the arrangement of tapes, as well as the optimized design of superconducting power cables based on YBCO-coated conductors, are investigated. According to the radial arrangement of the tapes, four different orientations of ferromagnetic substrate are considered: 1) out-in (substrate of inner/outer layer facing outward/inward), 2) in-out (substrate of inner/outer layer facing inward/outward), 3) in-in (substrates of both inner and outer layers facing inward), and 4) out-out (substrates of both inner and outer layers facing outward). We found that the AC loss of the superconducting layer for the out-in arrangement is the lowest. We also compare our calculations with experimental results.

Key words: High temperature superconductors, AC loss, power cable design, finite-element method

1. Introduction

High-temperature superconducting (HTS) power transmission cables, which have impressive properties, such as large electric transmission capacity, longer coverage distance, compact size, and above all low loss rates, are perfect candidates for transmitting electricity [1–4]. One of the main challenges in the utilization of HTS cables in power transportation is their high cost. The price of a first-generation (1G) wire for laboratory scale is approximately $300 per kA/m [5]. Moreover, the experimental setup for superconducting cables is very costly and time-consuming. Therefore, using the finite-element method (FEM) in the simulation of AC loss of superconducting power transmission cables, instead of experimental work, has been preferred by many researchers [6–10]. Simulations of cables have also been useful for predicting and understanding the measured loss mechanism for either transport or magnetization loss [11,12]. Comparison of AC losses for different gap widths, shapes of conductor, and widths and numbers of tapes in the HTS power transmission cables is also examined by means of FEM simulations [13–16].

*Correspondence: sukruyldz@gmail.com

The influence of the ferromagnetic (FM) material on the transport AC loss of HTS tapes, monolayer cables, and coils was extensively studied both experimentally and theoretically [17–23]. For the works on two-layer HTS cables made of coated conductors with a ferromagnetic substrate, Amemiya et al. [24] performed numerical AC loss calculations of two-layer superconducting power transmission cables comprising coated conductors with a ferromagnetic substrate concerning the arrangement with respect to the cable axis. Clem and Malozemoff [25] proposed a theory of AC transport loss in HTS power transmission cables made of second-generation (2G) wires with magnetic substrate. Experimental studies on AC loss of two-layer HTS power transmission cables made of 2G wires with a ferromagnetic substrate are presented in [26–28].

In this work, we investigate the impact of the tape arrangement on AC loss behavior of two-layer HTS cables with the idea that the magnetic field component normal to the superconductor layer depends strongly on the orientations of the ferromagnetic substrate. Through numerical simulations, we try to assess the effectiveness of designs in reducing the AC loss in HTS power transmission cables made with and without a ferromagnetic substrate.

2. General description of the model

In the present work, a two-dimensional (2D) model of the cable representing the cross-sectional view of coated conductors on the cable is utilized. In our 2D model, the coated conductors are considered to be infinitely long in the z direction, with their cross section in the $x-y$ plane. The model comprises three types of subdomains: a superconducting layer, the FM substrate, and the surrounding vacuum. For a nonmagnetic substrate, the substrate part is assumed to be a vacuum whose relative permeability (μ_r) is 1, while the electrical resistivity is very high. The helical structure of coated conductors along the cable axis is ignored; accordingly, whole coated conductors are assumed to be straight and parallel to the central axes of the cables: all layers are normal to the cross-section of the cables. The analyzed cable designs are displayed in Figures 1a–1e. The values given in [24] for the inner and outer radius of the cable are used. The gaps between two adjacent tapes in both interior and exterior layers are taken as 1.94 mm and 2.007 mm. The gap between adjacent tapes in each layer is determined by Eqs. (6)–(8) in [16], substituting the width of coated conductors w_{SC}, number of tapes N, and the inner, R_i, and outer, R_o, radii with the values in Table 1. We regarded only the $2\pi/N_{tape}$ part of the two-layer cable due to the periodicity in the cross-section. The specifications of the cables under analysis are given in Table 1. These are for a model using the actual thickness for the YBCO layer and including the FM substrate.

The influence of the tape arrangement and substrate magnetism on the AC loss of the power transmission cable is investigated using FEM analysis to figure out the mechanism leading to increased transport AC loss. The so-called A-V formulation implemented in the COMSOL Multiphysics package is adopted. The utilized software is suited to solve partial differential equations describing electrodynamics of materials. The basic electromagnetic equation involving magnetic vector potential is:

$$\vec{\nabla} \times \left(\frac{1}{\mu} \vec{\nabla} \times \vec{A} \right) = \vec{j} = -\sigma \left(\frac{\partial \vec{A}}{\partial t} + \vec{\nabla} V \right), \tag{1}$$

where μ is the magnetic permeability, $\vec{A}$ indicates the magnetic vector potential along the z axis, $\vec{j}$ is the overall current density, V indicates the scalar potential, and σ indicates the conductivity of the superconductor. Magnetic flux density $\vec{B}$ is connected to $\vec{A}$ by $\vec{B} = \vec{\nabla} \times \vec{A}$, and the electric field $\vec{E}$ is linked to magnetic vector

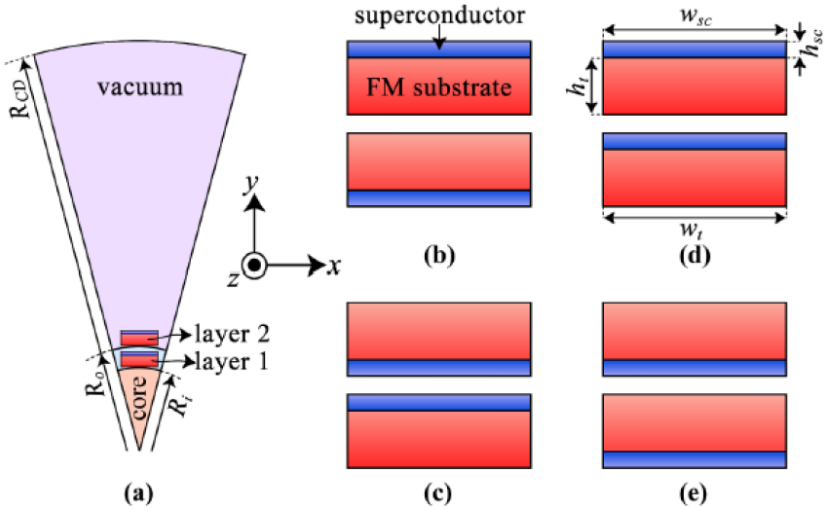

Figure 1. Rotationally invariant computational unit considered in FEM simulations (a), along with close-up views of the conductors laid in the out-in (b), in-out (c), in-in (d), and out-out (e) configurations. The conductors are not drawn to scale for clarity. The FM substrate configuration in (b)–(e) is such that the terms *in* and *out* denote the relative position of the substrate on layer 1–layer 2 with respect to the core.

Table 1. Physical and geometrical parameters adopted in the definition of HTS cables and in the implementation of FEM simulations.

Quantity (unit)	Description	Value
I_C (A)	The critical current in a cable	2400
A_n	Dimensionless scaling parameter for magnetic vector potential	2.0×10^{-8}
w_{SC}(mm)	Width of a conductor	4
h_{SC} (μm)	Height of a conductor	2
w_t(mm)	Width of ferromagnetic substrate	4
h_t (μm)	Height of ferromagnetic substrate	80
R_i (mm)	Inner radius of the cable	18.93
R_o (mm)	Outer radius of the cable	19.13
R_{CD} (cm)	Radius of the computational domain	$\sim 25\times$ R$_o$
N	Number of conductors in each layer	20
f(s^{-1})	Frequency of the applied current	50
T (s)	Period of the applied current	2πf

potential $\vec{A}$ and scalar potential V via

$$\vec{E} = -\frac{\partial \vec{A}}{\partial t} - \vec{\nabla} V. \tag{2}$$

The magnetic properties of the substrate part of a coated conductor are described by the constitutive equation:

$$\vec{B} = \mu \vec{H}. \tag{3}$$

Nonlinear $E - J$ relations like $E = E_c(J/J_c)^n$ have been implemented in the many commercial FEM software packages to solve Faraday (H-formulation) or Ampere (A-V formulation) equations [29,30]. Parameter n takes higher values than 20–25 for the coated conductors. Higher values of n can cause numerical instabilities,

particularly in the absolute critical state that may be attained if n goes infinity. In this work we propose an equation that gives the critical state and disregards overcritical states. To specify the characteristics of current density in the superconducting part, the following equation can be exploited [31–33]:

$$j_s = j_c \tanh\left(E/E_c\right). \tag{4}$$

Here, j_s is the current density in the superconductor, j_c is the critical current density, and E_c is the electric field criterion (e.g., 1 μV/m).

To avoid the complexity of the calculations, the constant critical density j_c for the superconductor and constant permeability for the ferromagnetic substrate have been adopted. Another part of the simulation is boundary setting. The boundary values for all boundaries have to be specified appropriately. Boundary conditions can be defined easily by using the magnetic potential boundary condition in COMSOL Multiphysics through its AC/DC module, thus ascertaining the vector potential at the outer boundary of the model. The analytical vector potential expression at any point (x,y) of distance from a long conductor with a rectangular cross-section carrying a uniform current density can be exploited as a boundary condition as given in [31,32]. The filaments are not electrically coupled and interact with each other only magnetically. Therefore, the constraint assigned in the finite-element calculation is that each cable layer transports the same amount of current I_{set}. This is carried out by adjusting the value of ∇V for every layer separately [32,34]. However, in the cross-section of one layer, the value of ∇V is constant. This is why inserting this constraint does not significantly increase the number of degrees of freedom in the solution process.

A mapped mesh technique has been utilized in the simulations for each superconducting layer with a much larger aspect ratio, where the tape width is divided into 700 slices, whereas its height comprises 15 elements, while the ferromagnetic layers comprise 1200 (width) $\times$ 8 (height) elements. A free triangular meshing is chosen for the calculation of the region outside of the coated conductor, which comprises 21,000 elements in the SC layers, 19,200 elements in FM layers, and 24,700 elements in the air subdomain outside of the cable cross-section. The total number of mesh elements is 64,900 and the number of total degrees of freedom is 96,705.

The total current is a sine function of time: $I(t) = I_{set}\ \sin\left(2\pi ft\right)$, where f and I_{set} are the frequency and the amplitude of the applied current, respectively. The total AC loss in the HTS layer is then determined by:

$$P_{sc} = \frac{1}{T}\int_0^T dt \int_S \vec{E}\cdot\vec{j}dS, \tag{5}$$

where T is the period of sinusoidal transport current and S is the surface area of the superconducting domain.

3. Verification of computational model

We finally compared our results with data extracted from the results reported in [26]. In both cases, the cable lies in the $x-y$ plane and the current flows in the z direction. For consistency, the cable is composed of $N_{tape} = 34$ coated HTS tapes, where the wrap pitch angle is $\theta = 20.9^\circ$. The cable arrangement is in the out-in configuration in Figure 1b. The calculated AC loss results in this work and in [26] are presented in Figure 2. For the comparison between our calculation method and the experimental data, along with the above values, we have exploited the field-dependent critical current density expression [18]:

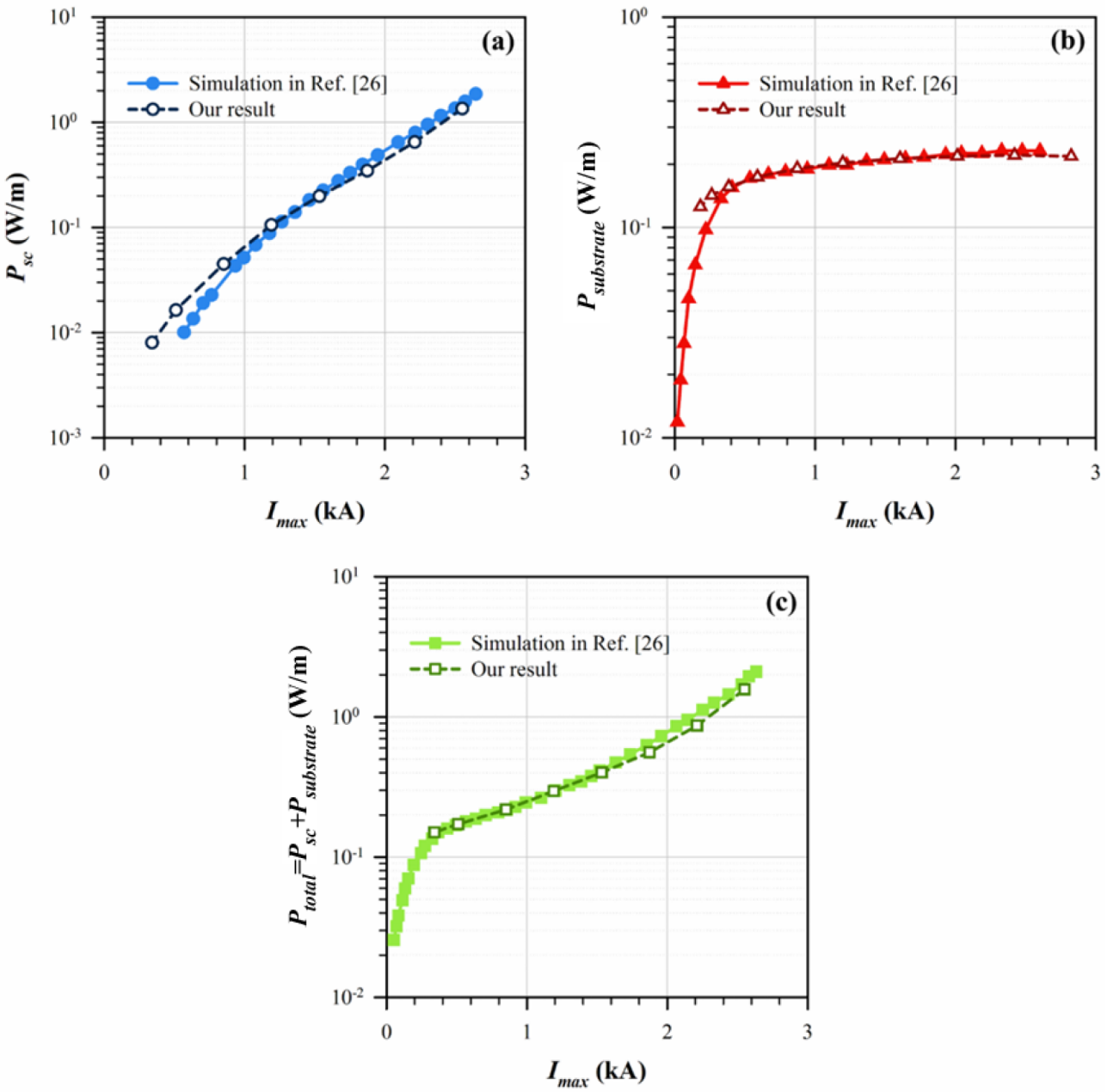

Figure 2. Comparison of AC power losses (in W/m) obtained in the present work (dashed lines, open symbols) with the results reported in [26] (solid lines, filled symbols) in the HTS tape (a) or substrate (b) parts of the cable, as well as the total losses (c) as a function of $I_{\max}$.

$$j_c = \frac{j_{c0}}{\left(1+\frac{\sqrt{k_a^2 B_{??}^2 + B_{\perp}^2}}{B_0}\right)^{\beta}}, \tag{6}$$

where J_{c0}, B_0, and β are the parameters assigning the features of the specific superconducting materials; k_a is the anisotropy parameter $k_a \leq 1$; and $B_{||}$ and $B_{\perp}$ are the parallel and perpendicular components of the

magnetic flux density to the wide surface of the tapes, respectively. The parameters in the calculation are given in Table 2.

Table 2. The parameters applied for the geometry and physical features of HTS cables and in the implementation of FEM simulations.

Quantity (unit)	Description	Value
I_C (A)	The critical current per conductor	100
α (deg)	Pitch angle	20.9
E_c(V/m)	Electric field criteria	1×10^{-4}
B_0	Critical current density parameter	0.36
β	Critical current density parameter	1.2
k_a	Anisotropy coefficient	1
w_{SC} (mm)	Width of a conductor	3.4
h_{SC} (μm)	Height of a conductor	0.8
w_t(mm)	Width of ferromagnetic substrate	4
h_t(μm)	Height of ferromagnetic substrate	75
R_i (mm)	Inner radius of the cable	15.50
L(μm)	The distance between the two layers	150
R_{CD} (cm)	Radius of the computational domain	$\sim 25\times$ R_o
N	Number of conductors in each layer	34
f(s^{-1})	Frequency of the applied current	50
T(s)	Period of the applied current	2πf
A_n	Scaling parameter for magnetic vector potential	10^{-8}

As clearly seen in Figures 2a–2c, the results are particularly consistent at higher current amplitudes. The discrepancy increases at smaller current amplitudes. The calculated value of the discrepancy at $I_{\max} = 500$ A between the results of two approaches is about 10%. The cause of this difference can be clarified by adjusting the constant critical current density (j_c) in calculation. Another factor could be physical effects, such as flux flow, which cannot be taken into account in simulations. The agreement for moderate $I_{\max}$ values is considerable. It should be noted that we have adopted flowing the same amount of current in both layers as a constraint, but, in fact, the magnitude of the currents could not be the same and uniform. The loss in the FM substrate is shown in Figure 2b. The calculation is carried out employing the formula given in [31]. A small difference between two results takes place at small $I_{\max}$. The total transport current losses are given in Figure 2c. The consistency between the two calculations is satisfactory.

4. Actual results

Comparison of evaluated total AC losses (Q_{sc}) in various conductor arrangements, where there exist $2N_{tape} = 40$ tapes, is introduced in Figure 3. A constant relative permeability (μ_r), which takes the value of either 1.0 or 5000, is assumed for all HTS tapes and nonmagnetic ($\mu_r = 1.0$) and ferromagnetic (FM) ($\mu_r = 5000$) substrates. The relatively high μ_r for the FM substrate is to clearly display its influences on the hysteresis loss. The loss in the cable with the nonmagnetic substrate is always smaller than in the case of coated conductors with FM substrate.

At small current amplitudes ($I_{\max}$ =10–30 A per tape), in particular, the total AC loss of the cable with nonmagnetic substrate is approximately 300 times smaller than in the out-in cable configuration, which exhibits the lowest loss among all FM-coated configurations. The FM substrate increases the normal component of the

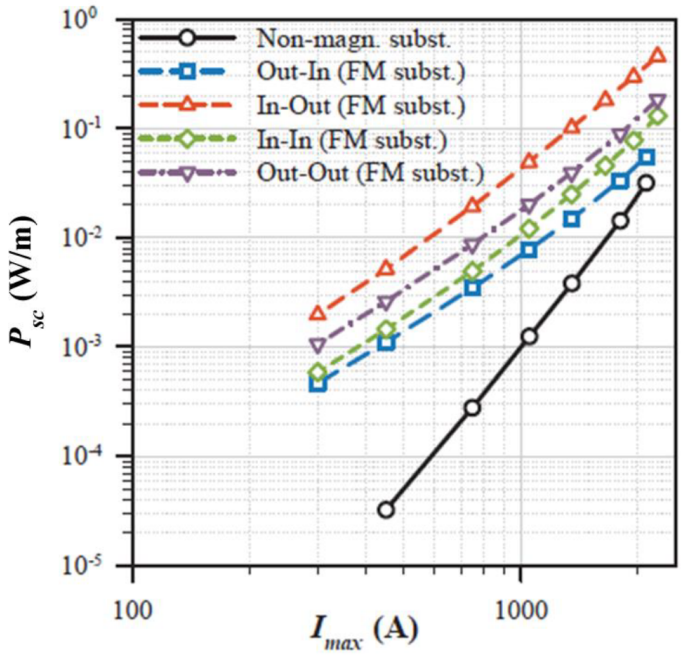

Figure 3. Comparison of transport AC losses between configurations depicted in Figure 1 for two-layer round HTS cables, for which $N_{tape} = 20$ in each layer. The μ_r of the nonmagnetic and FM substrates are taken as 1.0 and 5000, respectively.

self-field along the horizontal surfaces of the superconducting layer because of the concentration of magnetic flux in the substrate and thus leads to penetration of the field into the long face of the conductor.

When $I_{\max}$ approaches I_C, on the other hand, the transport AC losses of the conductors with the FM substrate are close to that of the conductors coated by a nonmagnetic substrate. Thus, it can be inferred that the AC transport loss is less affected by the magnetism of the substrate if the applied AC current amplitude is close to I_C. AC loss of the out-in configuration is always the lowest among all FM coating configurations. We note that the loss in the out-in configuration is approximately 10 times smaller than that in the in-out configuration if $I_{\max}$ is close to I_C.

The self-magnetic fields created by the two HTS tapes in Figure 1a are in opposite directions in the interior region between the tapes, while they are in the same direction in the outer regions (i.e. toward the core and vacuum in Figure 1a). Hence, the magnetic field is boosted/reduced in the outer/interior regions between the tapes. In the case of the out-in configuration in Figure 1b, where the substrates face each other, the magnetic field is almost eliminated in the interior space between layer 1 and layer 2 (L1 and L2), and thus less magnetic flux penetrates into substrates. Eventually, smaller loss occurs in this configuration. On the other hand, for the in-out configuration in Figure 1c, the substrates are situated in the exterior space, where they are exposed to an increased magnetic field. Consequently, much higher loss is encountered in this configuration. The loss of the in-in configuration in Figure 1d is approximately half of the loss in the out-out configuration in Figure 1e, as the HTS tapes are exposed to weaker magnetic fields.

To elucidate the AC loss mechanisms in the investigated cables, the loss curves are also obtained for individual L1 and L2 layers depicted in Figure 1a in FM coating configurations demonstrated in Figures 1b–1e and also in the case of a nonmagnetic substrate. The results presented in Figure 4 show that almost identical losses occur in L1 and L2 for the case of a nonmagnetic substrate. The situation is quite different in conductors

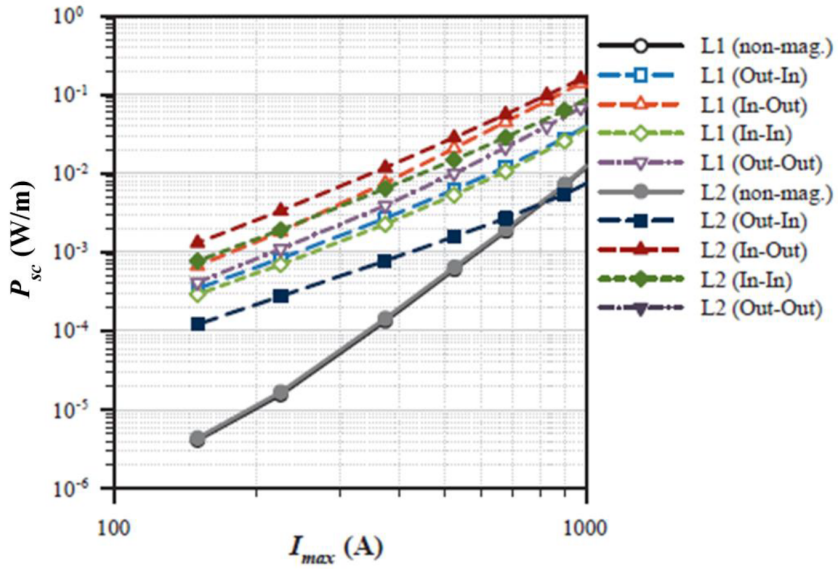

Figure 4. Comparison of transport AC losses in L1 and L2 when the HTS tapes are coated by either a nonmagnetic or FM substrate in configurations depicted in Figures 1b–1e.

with FM substrates. In the out-in configuration (see Figure 1b), the calculated AC loss in L1 is approximately three times higher than that in L2 at small $I_{\max}$. In contrast, when $I_{\max}$ approaches I_C, the ratio increases up to approximately 5. The situation is the opposite for the in-out configuration (see Figure 1c), whereas the discrepancy vanishes toward I_C. In the case of the in-in configuration (see Figure 1d), the AC loss curves of the out-out arrangement of L2 is overlapped on the L2 out-in, while L1 suffers higher loss in the out-out than out-in configuration (see Figure 1e). It seems that with the configuration depending on the FM substrate HTS tape design, the edge effect in the vicinity of both edges of the tapes can be diminished so that the long sides of the tapes in contact with the FM substrate transport more currents than the edges. The difference between the losses of the L2 layer in the out-in configuration and in the case of the nonferromagnetic substrate is remarkable at high current amplitudes, such as $I_{\max} = 0.9 I_C$.

Current distribution in 2D ($x - y$ plane) in L1 and L2 in HTS tapes coated with either nonmagnetic or FM substrate in one of the configurations in Figures 1b–1e is presented in Figure 5. It can be clearly seen that the edges of the tapes carry current with an opposite sign (in the -z direction) for small $I_{\max}$ for the nonmagnetic coating, whereas for FM substrates, the central parts of the HTS tapes contacting the substrate also carry current with an opposite sign. This is due to the fact that the generated self-field because of the FM substrate arrangement is higher and also penetrates more throughout the surfaces of the superconducting tapes (Figure 6). The current penetration at the edge of the tape on L2 in the out-out configuration is slightly less deep than those in other cable configurations with or without the FM substrate. This situation corresponds to minimum in the curves of AC loss.

Figure 6 displays the magnetic field distribution around the coated conductors in the cable at the same time instant and current amplitude, where large magnetic flux density is concentrated in the substrates exposed to the magnetic field caused by the current flowing in the superconducting layer. Consequently, the normal component of the flux lines at the tape faces is enhanced and causes large magnetic pressure on the superconducting strands. This leads to a greater amplitude of induced electrical field and brings about more power loss.

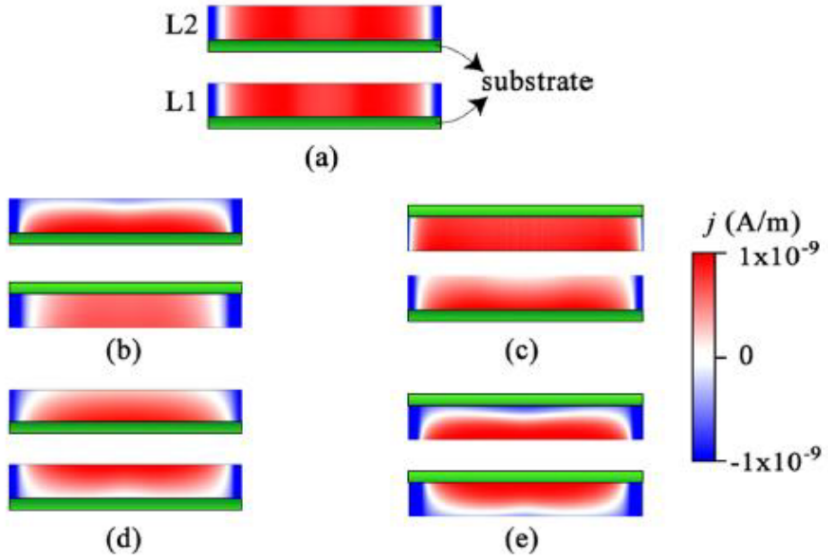

Figure 5. The 2D distribution of the current density (j) over the cross-section of HTS tapes lying in the $z-$plane are shown for $t = 3T/8$. Note how the presence of the strong FM substrate changes the current distribution inside the superconducting layers when carrying the same amount of current. Both L1 and L2 cable layers conduct an AC transport current of 16 A (about $I_C/5$) at $f = 50$ Hz for a nonmagnetic substrate (a) or a FM substrate in the out-in (substrate of the L1 and L2 layers facing radially outward and inward, respectively) (b), in-out (substrate of the L1 and L2 layers facing radially inward and outward, respectively) (c), out-out (substrates of both layers facing radially inward) (d), and in-in (substrates of both layers facing radially outward) (e) configurations. Neither the HTS tapes nor the substrates are drawn to actual scale. For the sake of clarity, the superconducting layer is shown much larger than real dimensions but the substrates are depicted narrower.

5. Conclusion

Using numerical simulations through the finite-element method, we have compared AC loss behaviors of two-layer round high-temperature superconducting cable models, in which the HTS tapes are coated either by nonmagnetic or strong ferromagnetic substrates. Calculation results showed that AC current transport losses and the current distribution depend strongly on the magnetism of the substrate and the arrangement of tapes when conductors are assembled cylindrically. The obtained results revealed that:

1) The AC loss in the two-layer HTS cable designed with nonmagnetic substrates is the lowest as compared to that of the conductors with ferromagnetic substrate.

2) The loss in the cable designed with ferromagnetic substrates is the lowest when the superconducting layer is in the out-in substrate configuration. However, the highest loss takes place when the tapes are in the in-out arrangement.

3) Although the losses evaluated in the inner and outer layers of the HTS cable designed with a nonmagnetic substrate are almost identical, discrepancy appears in the case of the ferromagnetic substrate. The lowest loss is encountered in the outer layer of the out-in tape arrangement.

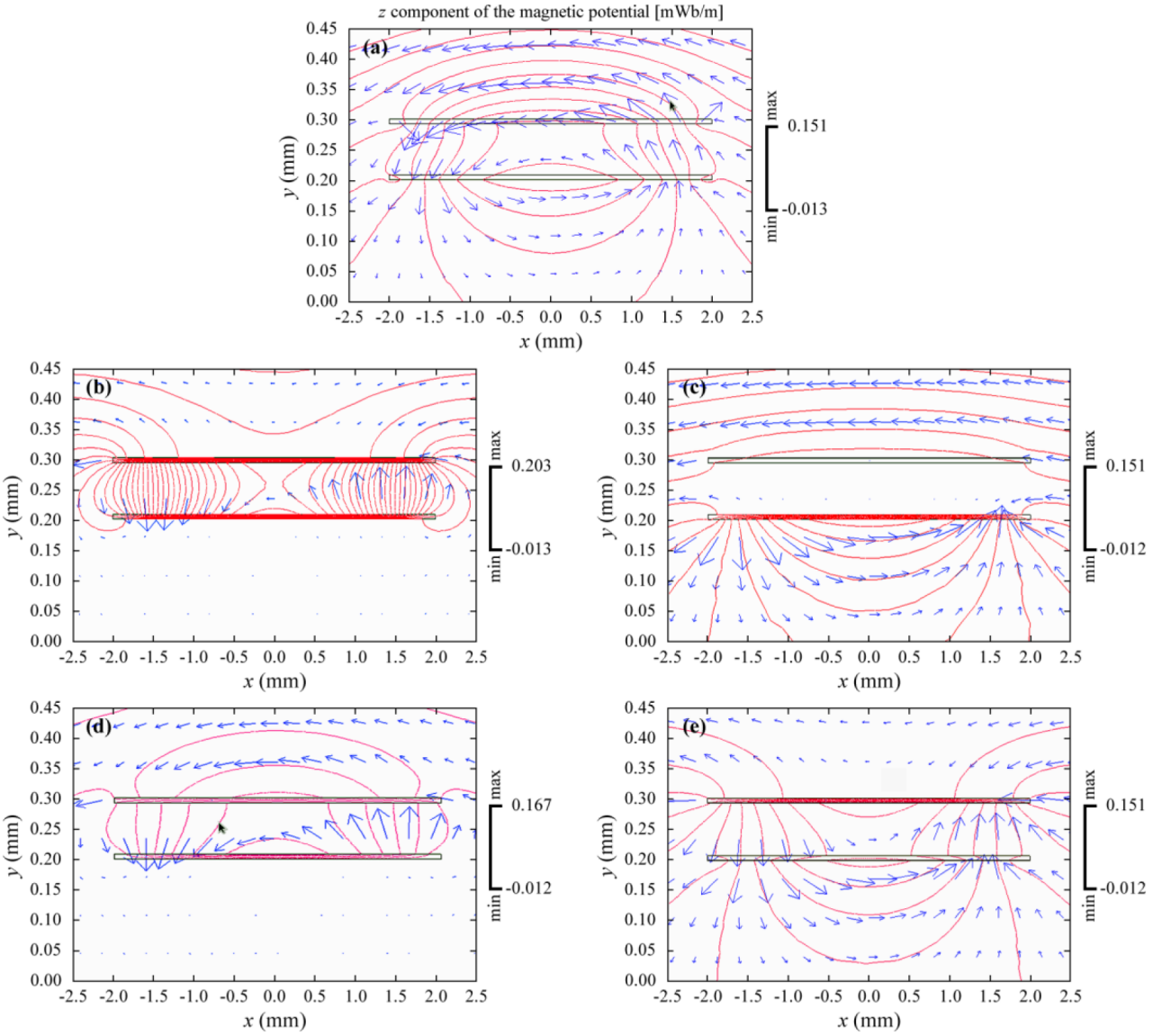

Figure 6. Contour plot of the magnetic vector potential representing flux lines around 1/20 parts of cable strands at the phase of applied current at time $3T/8$. The arrows represent the magnetic field direction.

Acknowledgment

This work was fully supported by the Scientific and Technological Research Council of Turkey (TÜBİTAK) under grant number 110T876.

References

[1] Masuda T, Yumura H, Ohya M, Honjo S, Mimura T, Kito Y. Design study of a HTS cable in Yokohama project. Phys C Supercond 2009; 469: 1702-1706.

[2] Demko J, Sauers I, James D, Gouge M, Lindsay D, Roden M, Tolbert J, Willen D, Trholt C, Nielsen CT. Triaxial HTS cable for the AEP Bixby project. IEEE T Appl Supercon 2007; 17: 2047-2050.

[3] Yumura H, Ashibe Y, Itoh H, Ohya M, Watanabe M, Masuda T, Weber C. Phase II of the Albany HTS Cable Project IEEE T Appl Supercon 2009; 19: 1698-1701.

[4] Sohn S, Lim J, Yim S, Hyun OB, Kim HR, Yatsuka K, Isojima S, Masuda T, Watanabe M, Ryoo H et al. The results of installation and preliminary test of 22.9 kV, 50 MVA, 100 m class HTS power cable system at KEPCO. IEEE T Appl Supercon 2007; 17: 2043-2046.

[5] Paranthaman MP, Izumi T. High-performance YBCO-Coated superconductor wires. MRS Bulletin 2004; 29: 533-589.

[6] Terzieva S, Vojenciak M, Pardo E, Grilli F, Drechsler A, Kling A, Kudymow A, Gömöry F, Goldacker W. Transport and magnetization AC losses of ROEBEL assembled coated conductor cables: measurements and calculations. Supercond Sci Technol 2010; 23: 014023.

[7] Siahrang M, Sirois F, Grilli F, Babic S, Brault S. A new numerical approach to find current distribution and AC losses in coaxial assembly of twisted HTS tapes in single layer arrangement. J Phys Conf Ser 2010; 234: 022034.

[8] Zhang M, Coombs TA. 3D modeling of high-T_c superconductors by finite element software. Supercond Sci Technol 2012; 25: 015009.

[9] Siahrang M, Sirois F, Nguyen DN, Ashworth SP. Assessment of alternative design schemes to reduce the edge losses in HTS power transmission cables made of coated conductors. Supercond Sci Technol 2012; 25: 014001.

[10] Takeuchi K, Amemiya N, Nakamura T, Maruyama O, Ohkuma T. Model for electromagnetic field analysis of superconducting power transmission cable comprising spiraled coated conductors. Supercond Sci Technol 2011; 24: 085014.

[11] Hamajima T, Tsuda M, Yagai T, Ozcivan AN, Shimoyama K, Aoyagi K, Soeda S. AC losses of a tri-axial superconducting cable with balanced three-phase current distributions. J Phys Conf Ser 2008; 97: 012253.

[12] Souc J, Gömöry F, Vojenciak M, Frolek L, Isfort D, Ehrenberg J, Bock J, Usoskin A, Rutt A. AC losses of a tri-axial superconducting cable with balanced three-phase current distributions. J Phys Conf Ser 2008; 97: 012198.

[13] Mawatari Y, Malozemoff AP, Izumi T, Tanabe K, Fujiwara N, Shiohara Y. Hysteretic ac losses in power transmission cables with superconducting tapes: effect of tape shape. Supercond Sci Technol 2010; 23: 025031.

[14] Malozemoff A, Snitchler G, Mawatari Y. Tape-width dependence of AC losses in HTS cables. IEEE T Appl Supercon 2009; 19: 3115-3118.

[15] Klincok B, Gömöry F. Influence of gaps in monolayer superconducting cable on AC losses. J Phys Conf Ser 2006; 43: 897.

[16] Li Q, Amemiya N, Takeuchi K, Nakamura T, Fujiwara N. AC loss characteristics of superconducting power transmission cables: gap effect and J_c distribution effect. Supercond Sci Technol 2010; 23: 115003.

[17] Souc J, Vojenciak M, Gömöry F. Experimentally determined transport and magnetization ac losses of small cable models constructed from YBCO coated conductors. Supercond Sci Technol 2010; 23: 045029.

[18] Vojenciak M, Souc J, Gömöry F. Critical current and AC loss analysis of a superconducting power transmission cable with ferromagnetic diverters. Supercond Sci Technol 2011; 24: 075001.

[19] Ainslie MD, Flack TJ, Campbell AM. Calculating transport AC losses in stacks of high temperature superconductor coated conductors with magnetic substrates using FEM. Phys C Supercond 2012; 472: 50-56.

[20] Mawatari Y. Magnetic field distributions around superconducting strips on ferromagnetic substrates. Phys Rev B 2008; 77: 104505.

[21] Zhang M, Kvitkovic J, Kim JH, Kim CH, Pamidi SV, Coombs TA. Alternating current loss of second-generation high-temperature superconducting coils with magnetic and non-magnetic substrate. Appl Phys Lett 2012; 101: 102602.

[22] Nguyen DN, Ashworth SP, Willis JO, Sirois F, Grilli F. A new finite-element method simulation model for computing AC loss in roll assisted biaxially textured substrate YBCO tapes. Supercond Sci Technol 2010; 23: 025001.

[23] Umabuchi M, Miyagi D, Takahashi N, Tsukamoto O. Analysis of AC loss properties of HTS coated-conductor with magnetic substrate under external magnetic field using FEM. Phys C Supercond 2008; 468: 1739-1742.

[24] Amemiya N, Nakahata M, Fujiwara N, Shiohara Y. AC losses in two-layer superconducting power transmission cables consisting of coated conductors with a magnetic substrate. Supercond Sci Technol 2010; 23: 014022.

[25] Clem JR, Malozemoff AP. Theory of AC loss in power transmission cables with second generation high temperature superconductor wires. Supercond Sci Technol 2010; 23: 034014.

[26] Vysotsky VS, Shutov KA, Nosov AA, Polyakova NV, Fetisov SS, Zubko VV, Sytnikov VE, Carter WL, Fleshler S, Malozemoff AP et al. AC loss of a model 5m 2G HTS power cable using wires with NiW substrates. J Phys Conf Ser 2010; 234: 032061.

[27] Fetisov SS, Zubko VV, Nosov AA, VPolyakova N, Vysotsky VS. Losses in power cables made of 2G HTS wires with different substrates. Phys Procedia 2012; 36: 1319-1323.

[28] Ohya M, Yumura H, Masuda T, Nagaishi T, Shingai Y, Fujiwara N. AC loss characteristics of RE-123 superconducting cable. J Phys Conf Ser 2010; 234: 032044.

[29] Coombs TA, Campbell AM, Murphy A, Emmens M. A fast algorithm for calculating the critical state in superconductors. Int J Comput Math Electr Electron Eng. 2001; 20: 240-252.

[30] Amemiya N, Miyamoto K, Banno N, Tsukamoto O. Numerical analysis of AC losses in high Tc superconductors based on E-j characteristics represented with n-value. IEEE T Appl Supercon 1997; 7: 2110-2113.

[31] Gömöry F, Vojenciak M, Pardo E, Souc J. Magnetic flux penetration and AC loss in a composite superconducting wire with ferromagnetic parts. Supercond Sci Technol 2009; 22: 034017.

[32] Gömöry F, Inanir F. AC losses in coil wound from round wire coated by a superconducting layer. IEEE T Appl Supercon 2012; 22: 4704704.

[33] Campbell AM. A new method of determining the critical state in superconductors. Supercond Sci Technol 2007; 20: 292-295.

[34] Henning A, Lindmayer M, Kurrat M. Simulation Setup for Modeling the Thermal, Electric, and Magnetic Behavior of High Temperature Superconductors. Phys Procedia 2012; 36: 1195-1205.